energies

MDPI

Article

Sizing and Allocation of Battery Energy Storage Systems in Åland Islands for Large-Scale Integration of Renewables and Electric Ferry Charging Stations

Jagdesh Kumar [1,*], Chethan Parthasarathy [1], Mikko Västi [2], Hannu Laaksonen [1], Miadreza Shafie-Khah [1] and Kimmo Kauhaniemi [1]

[1] School of Technology and Innovations, University of Vaasa, 65200 Vaasa, Finland; chethan.parthasarathy@uva.fi (C.P.); hannu.laaksonen@uva.fi (H.L.); miadreza.shafiekhah@uva.fi (M.S.-K.); kimmo.kauhaniemi@uva.fi (K.K.)

[2] Vaasan ammattikorkeakoulu, School of Technology, Electrical Engineering, University of Applied Sciences, 65200 Vaasa, Finland; mikko.vasti@vamk.fi

* Correspondence: jagdesh.kumar@uva.fi

Received: 21 December 2019; Accepted: 8 January 2020; Published: 9 January 2020



Abstract: The stringent emission rules set by international maritime organisation and European Directives force ships and harbours to constrain their environmental pollution within certain targets and enable them to employ renewable energy sources. To this end, harbour grids are shifting towards renewable energy sources to cope with the growing demand for an onshore power supply and battery-charging stations for modern ships. However, it is necessary to accurately size and locate battery energy storage systems for any operational harbour grid to compensate the fluctuating power supply from renewable energy sources as well as meet the predicted maximum load demand without expanding the power capacities of transmission lines. In this paper, the equivalent circuit battery model of nickel–cobalt–manganese-oxide chemistry has been utilised for the sizing of a lithium-ion battery energy storage system, considering all the parameters affecting its performance. A battery cell model has been developed in the Matlab/Simulink platform, and subsequently an algorithm has been developed for the design of an appropriate size of lithium-ion battery energy storage systems. The developed algorithm has been applied by considering real data of a harbour grid in the Åland Islands, and the simulation results validate that the sizes and locations of battery energy storage systems are accurate enough for the harbour grid in the Åland Islands to meet the predicted maximum load demand of multiple new electric ferry charging stations for the years 2022 and 2030. Moreover, integrating battery energy storage systems with renewables helps to increase the reliability and defer capital cost investments of upgrading the ratings of transmission lines and other electrical equipment in the Åland Islands grid.

Keywords: battery energy storage system; battery sizing; distributed generation; emissions; harbour grid; renewable energy sources

1. Introduction

Global trade proceeds to a large extent by the utilization of marine ships [1]. These marine ships can be considered as moving power plants, and their power capacity varies in the range of tens of megawatts [2]. Traditional ships mostly operate on fossil-fuels and create a significant amount of toxic emissions and air pollutions [3] during navigation and when staying at ports [4]. The international maritime organisation [1] and EU directives [5] have set targets and goals to limit environmental pollution and encourage cleaner sources of power generation for ships as well as

harbours. Conventionally, an auxiliary diesel engine generates electricity for ship services while staying at harbours. However, at present, an onshore power supply/cold-ironing is a preferred solution for ships to shut down their diesel engines at harbours to fill the requirements of strict emission regulations and make ports free from greenhouse gases [5,6]. Due to environmental reasons and new emission regulations, the power systems of ships and harbours are also shifting from non-renewable to renewable-based power generation. This will lead to the increased installation of renewable energy sources (RESs) and battery energy storage systems (BESSs) at ships and harbours [7]. At present, distributed generation (DG) is used to deploy electrical energy, especially from RESs, and is available in different forms and different scales, from the micro-scale to large-scale [8]. Wind and photovoltaic energy sources are gaining prominence, especially in harbour areas, to cope with the growing demand of modern hybrid and fully electric ships and ferries requiring an onshore power supply as well as charging stations. The integration of RESs into the harbour grid can be beneficial to avoid the expansion of the existing electrical network while supplying the additional power demand [2].

The modern ships operate either fully on electricity or with hybrid solutions and require their BESSs to be charged either from shipboard power systems or harbours. The all-electric ships [9] and all-electric hybrid vessels [10] require energy saving, energy efficiency and energy management systems for their integrated shipboard power system with the application of advanced power electronic converters [11], RESs and BESSs. The operation of the shipboard power system is also critical and prone to some technical issues regarding power quality [11] and power system protections [12]; therefore, BESSs are useful to mitigate power quality and reliability issues. Alternative harbour grid configurations have been proposed for the slow and fast charging of batteries for electric/hybrid vessels [13]. Modern ships require infrastructure in ports and harbour grids to be upgraded in order to facilitate the use of electric ships, enable the participation of harbour area microgrids in electricity markets [14,15] and benefit from the Internet of Maritime Things [16]. Therefore, the concepts of smart ports [17], wise ports [18], green ports [19], zero-emissions ports [20], and harbour area smart grids [4] deal with the design, operation and control of modern ports in such a way as to encourage power generation from renewables, manage and control power flow with flexible loads, and for charging and discharging the batteries at harbours [2,15]. Moreover, modern ports are not only consumers of electricity but also prosumers [21], using local generation from renewables to store energy and supply to the main grid if needed. However, intermittent power generation from renewables is a critical issue for the reliable operation of harbour grids; therefore, BESSs play a crucial role in balancing the power generation and demand by charging and discharging whenever needed, thereby providing flexibility in the power supply [22]. In order to utilise BESS efficiently, the challenging task is to optimally design the size and location of BESSs while keeping the future integration of RESs and load demand in mind [23,24]. In this way, the locally generated electricity from RESs could balance the load demand and power supply without expanding the power capacity of the overall network. At the same time, the future harbour grids could also anticipate a liberalised energy market to supply surplus power to utilities. In order to achieve the above-mentioned goals, an appropriate size of BESSs is required to be located at certain substations near harbours so that the power required at any substation could be uninterruptedly supplied.

Although the integration of RESs and BESSs has been considered by many researchers for shipboard power systems—although very few researchers have dealt with harbour grids—as depicted in Table 1, no researchers have considered the sizing and locations of BESSs for harbour grids while considering the integration of RESs and electric ferry charging requirements. The main contribution of this paper is to develop an algorithm which defines the proper size and power capacity of BESSs for any operational harbour grid planning for integrating RESs and electric ship and ferry charging stations locally without the expansion of the power capacity of transmission lines and other grid components. To the best of the authors' knowledge, and according to the literature surveyed so far, this is the first attempt to size and allocate BESSs on larger scale for any harbour grid, planning for the integration of a huge amount of RESs. In order to examine the proposed methodology, a real-world

system—the Åland Islands power system—is considered as the test case. On this basis, two future case studies are modelled in the Power Systems Computer-Aided Design (PSCAD) software, which plans a significant amount of RESs for the two horizon years of 2022 and 2030. The maximum loadings with a minimum integration of renewable power generation for the years 2022 and 2030 are taken as base cases, keeping future predictions in mind. The base cases are simulated in PSCAD without BESSs under maximum loading and minimum generation for the years 2022 and 2030. The simulation results are compared with the base case studies and validate that the batteries are accurately sized and located at a proper location to avoid the expansion of the power capacity of the transmission lines, transformers, and other protective electrical equipment in Åland's electrical network.

Table 1. Taxonomy of literature review. PV: photovoltaic; BESS: battery energy storage system.

Ref.	Year	Wind	PV	BESS	Onshore Power Supply	Battery-Charging Stations for Vessels	Port as Energy Market	Sizing of BESS	Allocation of BESS	Harbour Grid/Port Power Systems	Shipboard Power Systems
2	2019						✗	✗	✗		✗
3	2017						✗	✗	✗		✗
6	2013	✗			✗	✗	✗	✗	✗	✗	
10	2018	✗	✗		✗	✗	✗	✗	✗	✗	
12	2019						✗	✗	✗		✗
13	2019		✗	✗		✗		✗	✗		✗
14	2019	✗	✗	✗		✗		✗	✗		✗
16	2015				✗	✗		✗	✗	✗	
17	2016					✗		✗	✗		✗
19	2012					✗	✗	✗	✗		✗
20	2017		✗			✗	✗	✗	✗		✗

The rest of the paper is organised as follows. Section 2 provides insights for utilising lithium-ion (Li-ion) batteries for stationary applications, shows the importance of modelling their performance characteristics accurately, and explains the methodology of developing an algorithm for the proper sizing and location of BESSs on different substations of harbour grids considering RESs. Section 3 investigates the impacts of the proposed methodology, analyses the results for two different horizon years, and discusses the main findings and challenges in designing and allocating BESS at proper substations; finally, Section 4 presents the conclusions and future work.

2. Proposed Methodology for BESS Sizing and Allocation

Modern power systems are rapidly changing with the increased penetration of RESs and transportation electrification, including in the marine sector. Under such circumstances, BESSs play an important role in providing short-term flexibility for various stationary grid applications. It is necessary to understand and analyse the effects of such architectural changes on the stability and reliability of the grid. Considering the inherent characteristics and cost economics of BESSs, defining the role of BESSs and their sizing is essential. In this paper, a methodology is proposed for BESS sizing and allocation to mitigate line congestion (leading to capital deferral) for harbour grids. Figure 1 provides an overview of the technologies included in the study. Renewable energy sources such as photovoltaic (PV) and wind energy and the load consumption arising from ferry charging stations, residential consumption, and other related harbour loads are considered in the study. BESSs act as the main flexibility resources in the system. This section provides an overview of the characteristics and performance of Li-ion batteries, defining their capability to act as short-term flexibility resources in smart grids. It also explains the reason for accurately modelling Li-ion battery behaviour, by means of an equivalent circuit battery modelling methodology due to its highly non-linear voltage and current characteristics. This is followed by an algorithm which was developed to size and allocate BESSs for the stable operation of weak grids or harbour grids, catering for changes caused by increased renewable energy penetration and load consumption changes.

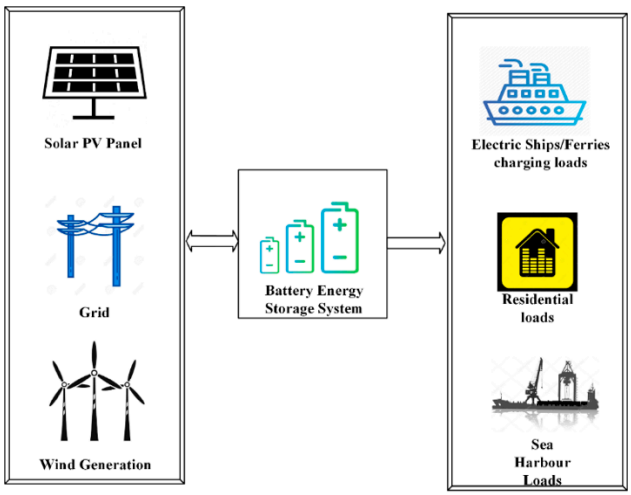


Figure 1. Technologies involved in the method.

2.1. Lithium-Ion Batteries

The large-scale integration of renewables and low-emission energy sources at all voltage levels—i.e., high, medium and low voltage—has followed a rising trend. Integrating such a large amount of variable and usually low-inertia renewable energy sources has significant impacts—predominantly voltage and frequency instabilities—compared to traditional centralized power systems. Due to these changes and effects, there is an increasing need for various type of energy storages for applications with different time-scales. For flexible energy needs, the interest in rapidly controllable Li-ion BESSs has increased due to their technological advancements and decreasing costs. The accurate modelling of battery packs for stationary energy storage grid applications has been minimal, as the majority of the literature considers battery systems as an ideal DC voltage source [25] or utilizes mathematical modelling techniques. Mathematically based kinetic battery models (KBM) were first proposed in [26] for lead-acid batteries. Modified KBMs [27] are widely used to simulate Li-ion batteries for smart grid simulations. However, KBMs fail to address the non-linear characteristics of Li-ion batteries, which are also affected by various operating conditions such as their State-of-Charge (SoC), temperature, current rate, and age.

Physics-based electrochemical models [28] are suitable to model the internal behaviour of the cell but involve a huge amount of mathematical computations, which makes them practically impossible to be used for smart grid simulations. The integration of an equivalent circuit model (ECM) has been presented for electrical vehicle propulsion in [29], considering SoC as the only impactful parameter. The ECM presented in [30] shows the battery characteristics of an electric vehicle with respect to aging under the World Motorcycle Test Cycle for electric vehicle battery characterization, tracking the internal resistance with one resistive–capacitive (RC) branch. The battery cell model, whose parameters are concerned with physical phenomena such as the effects of SoC and temperature, is explored in [31]. Most of the ECM models of BESSs reported for power system simulations lack one or several affecting parameters related to the performance of Li-ion batteries.

Battery design, sizing, the optimisation of control, and dispatch strategies are more likely to succeed when they are based on more accurate BESS models. Also, there is an urgent need for accurate battery performance models because modern battery management systems rely on such models to track the key parameters of each cell and the whole battery energy storage system. In this paper, a detailed ECM of Li-ion BESSs is presented, and secondly, the developed model is used to accurately size a BESS for different locations and substations in the Åland Islands as a case study to avoid network congestion and defer capital investments in terms of upgrading the network size.

2.2. Modelling Lithium-Ion BESS

Their ability to react quickly, as well as their higher energy and power density, longer cycle and shelf life, low rate of self-discharge, high round trip efficiency and improved safety performance, have meant that Li-ion BESSs have been favoured for stationary grid applications. Li-ion BESSs are capable of acting as flexible energy sources and provide multiple technical ancillary services such as load levelling, peak shaving, islanding/microgrid operation, black start support, network loss minimization, frequency support, and voltage regulation.

Li-ion batteries are intercalation-based energy storage systems which operate as a closed system [32] with very few measurable state variables, making it difficult to properly monitor the states of the battery and maintain safe operation. Voltage, current and temperature measurements are typically used to determine or estimate all other parameters of the battery—typically its SoC and state-of-health. Therefore, it is necessary to understand and precisely model the behaviour of the BESS under various operating conditions.

The Thevenin-based second-order equivalent circuit (SOEC) model is a versatile technique, as it successfully emulates model parameters such as the multi-variable SoC, charge-rate (C-rate), temperature, hysteresis effects, self-discharge and battery aging. SOEC is considered as the benchmark model for Li-ion batteries, as it depicts the charge transfer, diffusion and solid electrolyte interface reactions in the form of resistors and capacitors. The SOEC battery model presented in [33] is based on time domain measurements from hybrid pulse power characterization tests, whose performances are affected by the SoC, operating temperature, C-rate and aging of BESSs. Therefore, the developed SOEC model presents a perfect balance between the accuracy and complexity of battery modelling. Figure 2 shows the proposed dynamic equivalent circuit model for a nickel–cobalt–manganese-oxide (NMC) type Li-ion battery cell. The Open Circuit Voltage (OCV) is modelled as an ideal voltage source, and the internal resistance is modelled as R_i. Two RC combinations are suggested for modelling the Li-ion battery cell, meaning that the dynamic behaviour is modelled as R_1, C_1, R_2 and C_2. The hysteresis effect and polarization effect in the Li-ion cells can be simulated accurately enough with the two RC combinations, and the model structure is simpler compared to more RC combinations. As the actual behaviour of the NMC battery cells is significantly non-linear, all the parameters vary with the SoC, temperature, age and history (number and depth of cycle) of the cell. OCV, R_i, R_1, C_1, R_2, and C_2 are the parameters obtained from the experimental characterization of the lithium-ion battery cell at various SoCs (100% to 0% with a step of 10%), temperatures (15 °C, 25 °C, and 45 °C), C-rates (1C, 2C and 3C) and cycle ages (0, 100, 500, 1000, 1500, and end of life). V refers to the battery cell terminal voltage.

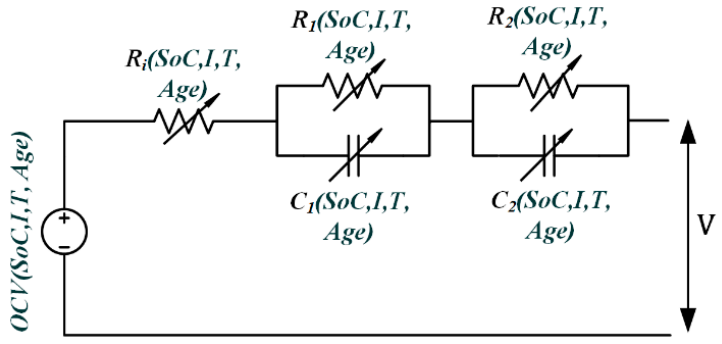


Figure 2. Second-order equivalent circuit (SOEC) battery cell model.

Figure 3 provides a comparison between the simulated and experimental discharge voltages at different aging levels of the NMC battery cell, at a 25 °C and 3C discharge rate, that were recorded as a result of accelerated aging tests. The mathematical representation of the output voltage characteristics for the second-order ECM is given in [33], and the SoC is estimated by the coulomb counting method [34].

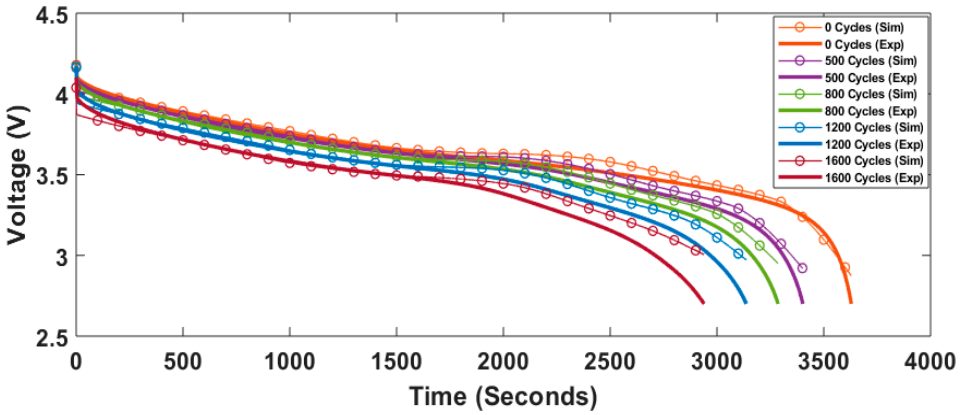


Figure 3. Comparison between simulated and experimental cell discharge voltages with different aging intervals.

The mean relative error was less than 2% for the majority of the discharge cycles, but in some cases (especially at higher aging), the error was greater than 5% towards the end of discharge. It is evident that the overall discharge capacity reduces with aging, which in turn reduces the overall discharge time. The performance of Li-ion BESS changes drastically with aging; thus, the overall discharge energy from the batteries reduces with aging. Predicting the accurate state of energy (SoE) of batteries will aid in the improved design of battery management systems (BMSs) and their respective energy management systems (EMSs). In this study, batteries were considered at their beginning of life to derive the battery size for harbour area smart grids. Hence, modelling the aging characteristics of batteries is a critical task for smart grid applications, because the energy/power status of the BESS is required in order to consider its capability for supplying active power (P) and to provide ancillary services such as frequency support or peak shaving.

2.3. Lithium-Ion BESS Grid Integration

A typical topology for the integration of BESS in utility grid applications is presented in Figure 4, which is deployed as a reference for the battery sizing algorithm presented in the next subsection. The nominal BESS voltage ($V_{DC,BESS}$) is considered as 600 V, which is connected to the DC bus. The DC/AC converter connected with the DC bus converts 600 V_{DC} power to three-phase, 400 V_{RMS} AC power. In the Åland Island case, the voltage will be boosted to a 10 kV level by means of a three-phase transformer. The allocation of BESSs in the substation is designed from the voltage, current and power flow data obtained from PSCAD EMT simulations. Results from the simulation provides data input on loading information of each power transmission line and the status (i.e., voltage levels and current flows) at every operational substation.

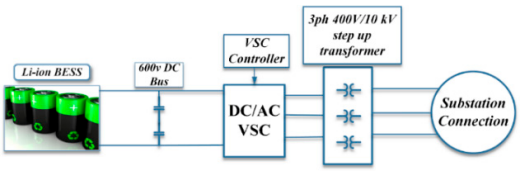


Figure 4. BESS grid integration topology.

2.4. Battery Sizing and Allocation Algorithm

Figure 5 provides a methodology of Li-ion BESS sizing for weak networks/harbours in order to integrate more electric ferry/ship charging stations and RESs. The proposed methodology has been employed in the Åland Islands to reduce or eliminate network congestion and capital investment to upgrade the existing power transmission lines by installing BESSs at critical locations. The line current data obtained from the base case studies of PSCAD simulations are the primary input for this algorithm.

The line current ($I_{,LINE}$) along with the maximum line current capacity (I_{Max}) for each transmission line of 45 kV are provided as input to the algorithm. If $I_{LINE} < I_{Max}$ for a certain transmission line, then the power transmission line is not under congestion.

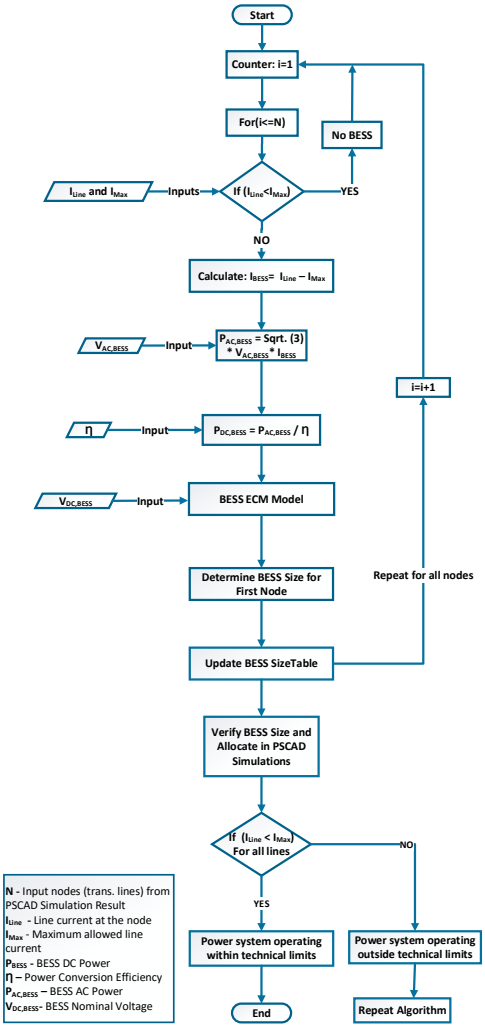


Figure 5. Battery sizing and allocation algorithm. ECM: equivalent circuit model. PSCAD: Power Systems Computer-Aided Design.

However, if $I_{LINE} > I_{Max}$, then that transmission line is under congestion, and there is a need for the installation of BESS in the adjoining substation. Further, the relevant sizing of the Li-BESS for grid applications is imperative considering its economic and environmental burden for a project. The battery cell ECM model aids in the accurate sizing of BESSs for power grid applications. In the later part of the algorithm, The BESS AC voltage ($V_{AC,BESS}$) is given as an input to calculate the BESS AC power ($P_{AC,BESS}$). In the next step, DC power requirements from BESS ($P_{DC,BESS}$) are computed by providing the converter power conversion efficiency, η (95%)as an input. Further, the required BESS nominal voltage ($V_{DC,BESS}$) and $P_{DC,BESS}$ are given as inputs to the developed ECM model. Based on the project requirements, performance-affecting parameters such as the temperature, SoC, age, and current ratings are introduced in the battery model. Based on $V_{DC,BESS}$ and $P_{DC,BESS}$, the battery size at a particular substation is calculated. The parameters of the battery size include the number of series cell connections (N_s) to attain the required nominal voltage levels and the number of parallel string connections (N_p) to obtain required current-carrying capacity, peak discharge power and energy, nominal discharge power and energy characteristics, and nominal charging power requirements. The algorithm then continues on to the next input I_{LINE} until all the inputs are completed. By this method,

the optimum Li-ion BESS size at the required substation is determined precisely. Further, the designed BESS is allocated to the selected substations in the PSCAD model of the Åland Islands to perform EMT simulations and record I_{LINE}. In a case in which the transmission lines are still being overloaded (i.e., $I_{LINE} > I_{Max}$), the algorithm in Figure 5 will be reiterated until the right BESS size is obtained.

3. Numerical Studies

This section introduces a real-world test case of a harbour grid in the Åland Islands, which has been simulated by considering future targets of integrating more electric ferry/ship charging stations and RESs with the utilization of BESSs for the years 2022 and 2030. The simulation results and a discussion of the findings are also given in this section.

3.1. Real World Test Case

The geographical location of the grid structure of the Åland Islands, located in the Baltic Sea in Finland, is shown in Figure 6, and a simplified single line diagram is shown in Figure 7. There are two power transmission lines of 110 kV supplied from Senneby (Sweden) and Nådendal (Finland). In addition to the 110 kV transmission lines, two other power transmission lines of 45 kV are supplied from Båtskär (wind park) and Gustavs (Finland). Senneby is an HVAC (high voltage alternating current) transmission line, which is the main power supply for the whole network, whereas Nädendal is an HVDC (high voltage direct current) transmission line, which is used as a backup power supply for the network. Bätskär and Gustavs have weak grid connections because of the intermittent nature of the power supplied from wind power generation. The Föglö substation is currently not operational, but keeping in mind the future marine load demand and integration of renewables, it will be installed between Svinö and Sottunga substations. Moreover, each 45 kV substation is also connected to a 10 kV substation with step down transformer(s) of 45/10 kV to supply marine and other harbour loads. The Åland Islands grid is a quite small and weak power system with many potential medium-size/small harbour areas for future ferry/ship charging stations and the integration of a large amount of RESs. Electric ferries are used for transportation between multiple islands. Typically, the Åland Islands grid is supplied with power from Sweden and Finland. Åland's power system has several substations with different load requirements and the possibility of more than one topology for connecting one substation to another substation. Regarding future load demand, Åland Islands stakeholders are planning to integrate a large amount of renewables (photovoltaic and wind power) in the years 2022 and 2030 with targets to electrify transportation in the main island and between multiple islands. Therefore, significant development in the power system's infrastructure will be needed. This development is considered in two phases for the years 2022 and 2030, which will encounter an increase in the penetration of renewables as well as power demand from electric ferries/ships requiring an onshore power supply and the recharging of on-board batteries at harbours.

To analyse the effectiveness of integrating BESS, the base case and two future case studies for the years 2022 and 2030 have been simulated with the detailed simulation models developed in Power Systems Computer-Aided Design (PSCAD). The base case simulation model considers the maximum loading for the years 2022 and 2030, but without the integration of renewables and BESS, whereas simulation models for the case studies for the years 2022 and 2030 consider the implementation of BESS as well, and they present the effect of the integration of the minimum and maximum number of BESSs on network topologies. The following subsections explain the simulation results obtained from the base case, 2022 case, and 2030 case.

3.2. Simulation Results and Analysis

This section explains the results of base case studies without considering BESSs, and then compares and analyses the results with the integration of BESSs in future case studies for the years 2022 and 2030. For each case study, radial and meshed network topologies have been considered, because the

radial topology is the current operational scenario of the Åland Islands power system, and the meshed topology, when compared to the radial, has generally following advantages:

(1) It is more resilient against faults (the electricity supply reliability is better, because customer loads/generated power can be fed from two-directions instead of only one).
(2) The voltage level can be maintained more stably with a meshed topology in different distribution network points (the DG hosting capacity can be typically increased with meshed topology).

However, protection is typically somewhat more complex with meshed than radial networks.

3.2.1. Base Case Studies for 2022 and 2030 without BESS

The base case is simulated to investigate the operation of the Åland Islands electricity network for future predicted marine load demands for onshore power supply and ferry charging stations for the years 2022 and 2030, but without integrating renewables and BESSs. This enables us to examine which transmission lines and other electrical equipment, such as transformers and protective devices, are overloaded. Since the focus of the paper is to design a BESS of a proper size and allocate it at the required substations, only the details regarding the overloading of transmission lines and voltage levels at all the substations of 45 kV are of interest in this paper. The power system in the Åland Islands is operated typically as a radial network, with the following circuits breakers between the substations in open positions: Västanträsk and Storby, Finby and Svinö, Svinö and Föglö, Norrböle and Mariehamn.

The minimum generation and maximum loading cases for 2022 and 2030 are considered in such a way that power supplies from Bätskär and Nådendal are not operational in the simulation model. By considering the above operational criteria along with the predicted load demand for the years 2022 and 2030, the basic single line diagram of the simulation model is shown in Figure 8. Thus, the current operation of power system in the Åland Islands can form two possible islanded sections of the network in radial topologies.

The estimated capacity of power generation from solar photovoltaic sources in 2022 is 33 MW by 3 MW equally at all 10 kV substations, and 30 MW of wind power at Tellholm substation, totalling 63 MW, whereas the estimated capacity of power generation from the integration of renewables in 2030 is 143 MW with reference to year 2022 by installing a photovoltaic source of 10 MW at Hellesby, 118 MW of wind power at Föglö and a 15 MW increase in the power capacity of wind power already installed at Tellholm. A huge amount of power will be generated by RESs, which will replace the grid power supplied from Senneby, Nådendal, and Gustavs substations. The base case simulation shows that it is a challenging task to provide an uninterrupted power supply due to intermittent nature of the power supply from renewables. Therefore, this provides a basis for the installation of a suitable size of BESSs at suitable locations for efficient and stable grid operation. Moreover, the BESSs are supposed to be charged in off-peak time, and especially from the local power generation from renewables, and discharged whenever there is a peak load demand.

The detailed model of the Åland Islands' electricity network is first simulated for the base case in PSCAD without BESSs, and then the line currents along with their maximum current-carrying capacity are fed to an algorithm developed in MATLAB/Simulink, which is used to accurately size the BESS as described in Section 3. Moreover, some techniques are also adopted for controlling the reactive power so that the voltage at different substations remains within the limits, as shown in Figure 9. However, the current flowing for some lines exceeds the upper limits of the current-carrying capacity, as shown in Figure 10. Therefore, BESSs have to be located in those substations to decongest the network and reduce power losses and improve the system stability in the network. The following case studies for the years 2022 and 2030 are carried out in the following subsections, which show that a BESS can reduce the upper limits of the current-carrying capacity of those transmission lines.

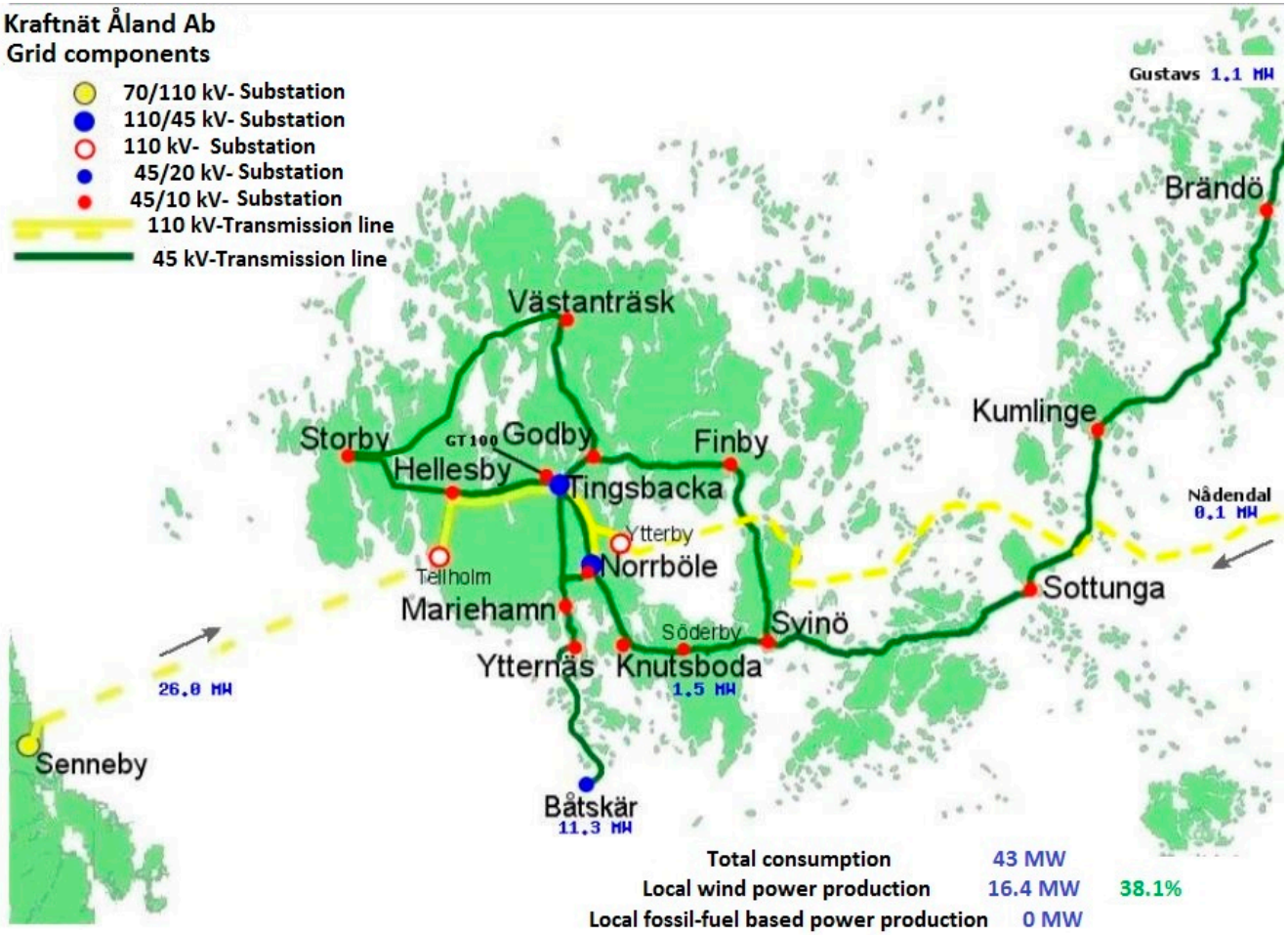
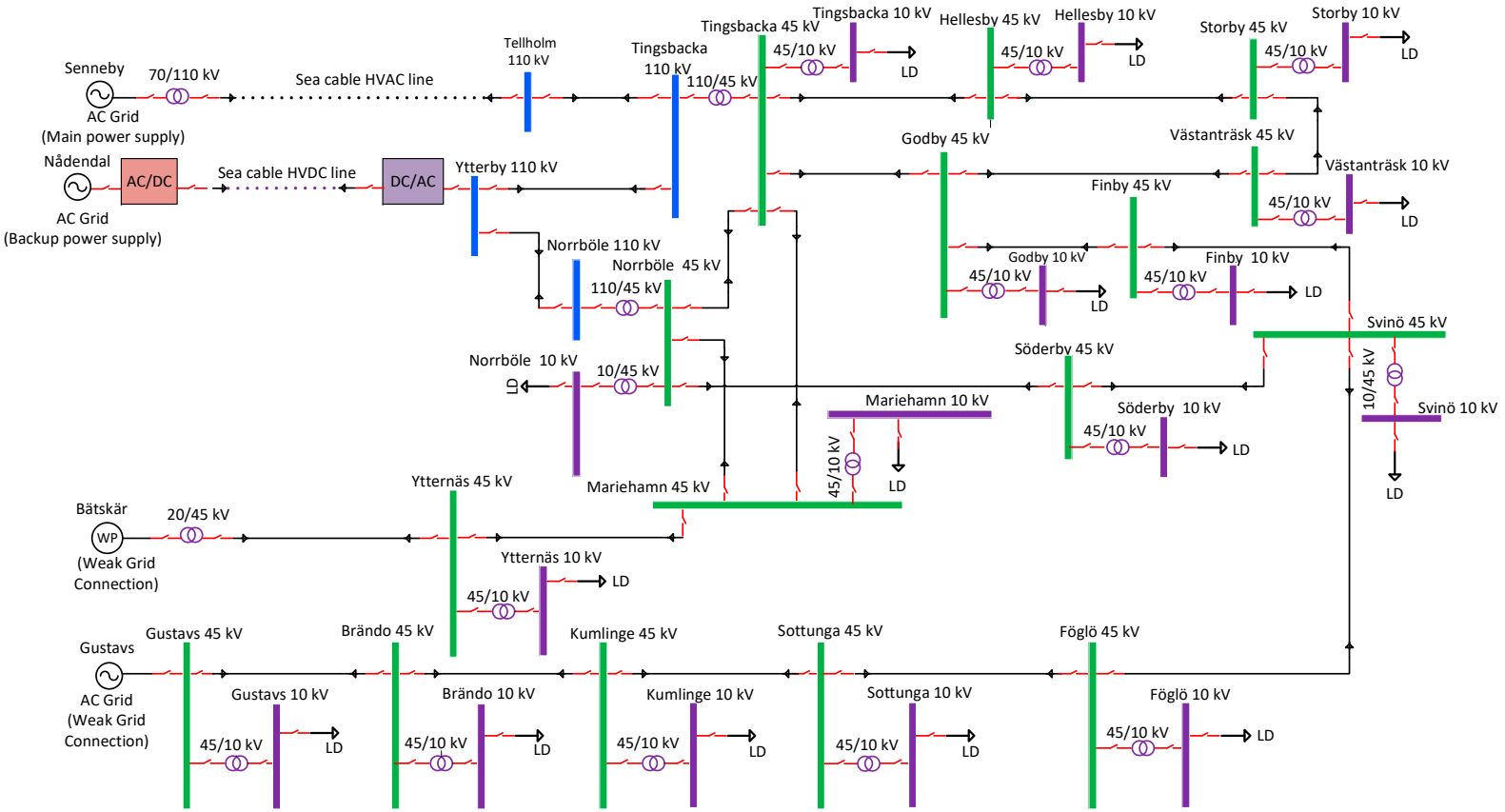


Figure 6. The geographical location and grid structure of the Åland Islands [35].



AC = Alternating Current
DC = Direct Current
HVAC = High Voltage Alternating Current
HVDC = High Voltage Direct Current
LD = Load Demand
WP = Wind Power

Figure 7. Single line diagram of the Åland Islands' power system.

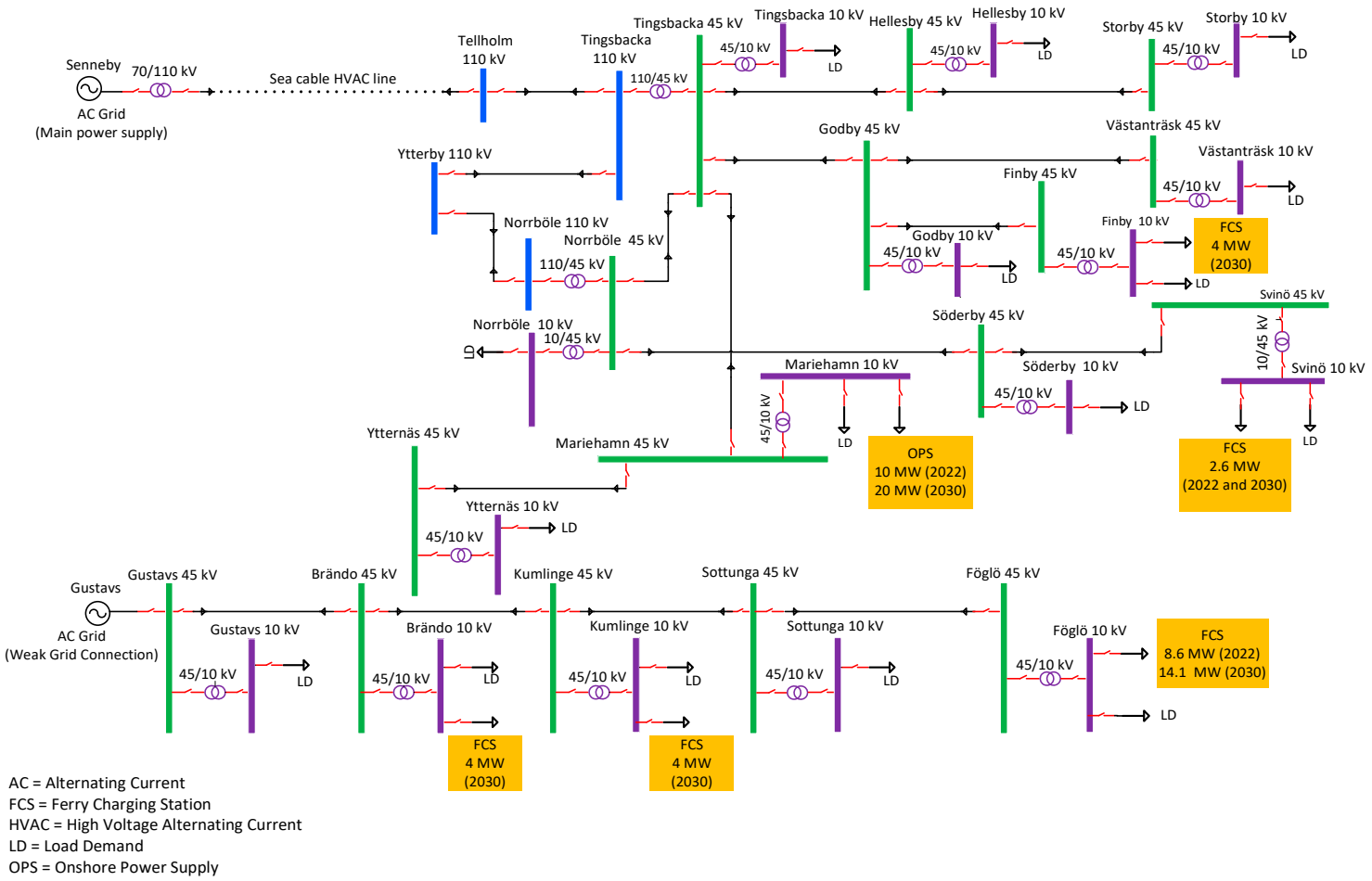


Figure 8. Single line diagram of the electricity network in thr Åland Islands for base case studies without BESSs.

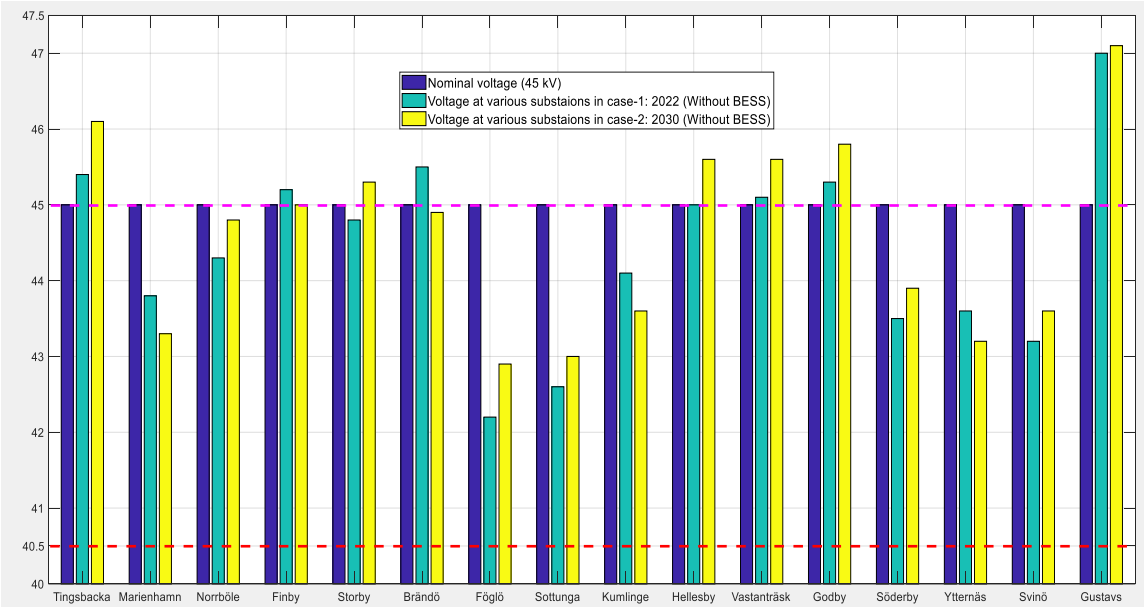


Figure 9. Nominal and operating voltages at the substations in the base case.

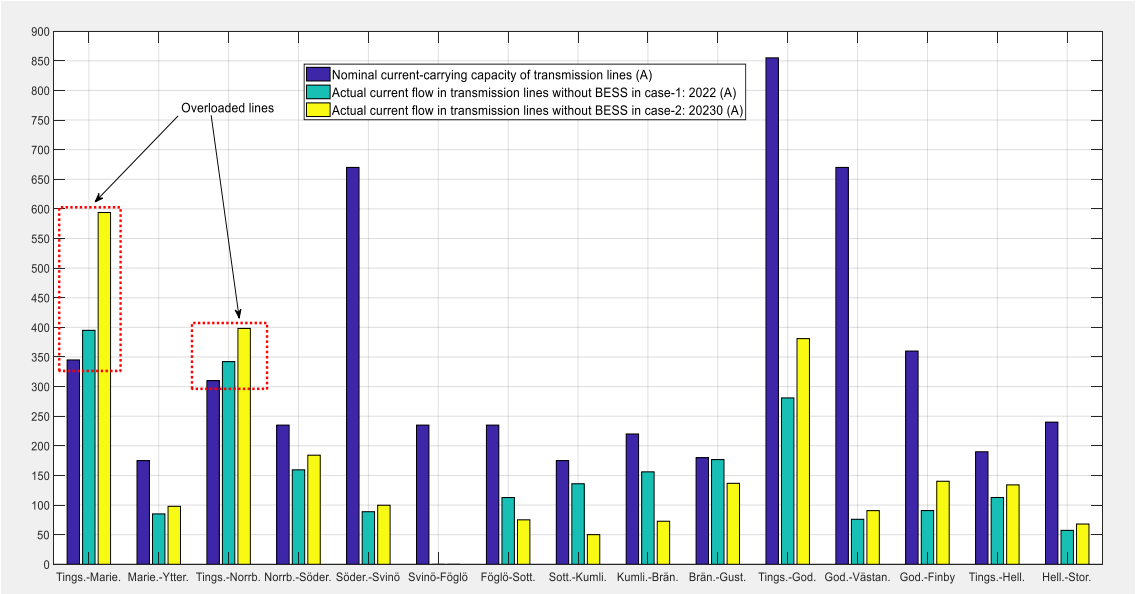


Figure 10. Nominal and actual current flow in transmission lines in the base case study.

3.2.2. Case 1: Year 2022 with BESSs

In the case of 2022, a BESS has been integrated into two network topologies: one is the present operating scenario—i.e., the radial network—and the other is a meshed network by considering the upper islanded network supplied by Senneby. Figure 11 shows the radial network topology with the total predicted increase in load demand of 21.2 MW with reference to the present-day load demand, and this has been distributed at Mariehamn, Svinö, and Föglö substations. In this network topology, the appropriate size of the BESS was found to be of 5 MVA each, and the strategic locations were at Mariehamn, Norrböle and Föglö substations. Figure 12 illustrates the meshed network topology with the same increase in load demand of 21.2 MW, distributed at Mariehamn, Svinö, and Föglö substations. In this network topology, the suitable size of the BESS was found to be 2.5 MVA each, and the strategic locations were at Mariehamn, Norrböle, and Föglö substations. Figure 13 shows the nominal voltage profiles of 45 kV substations' operating voltages without BESSs and with BESSs in radial and meshed

network topologies. It has been verified that the voltage profiles have slightly improved with the integration of BESS, and they are within the limits of ±10%.

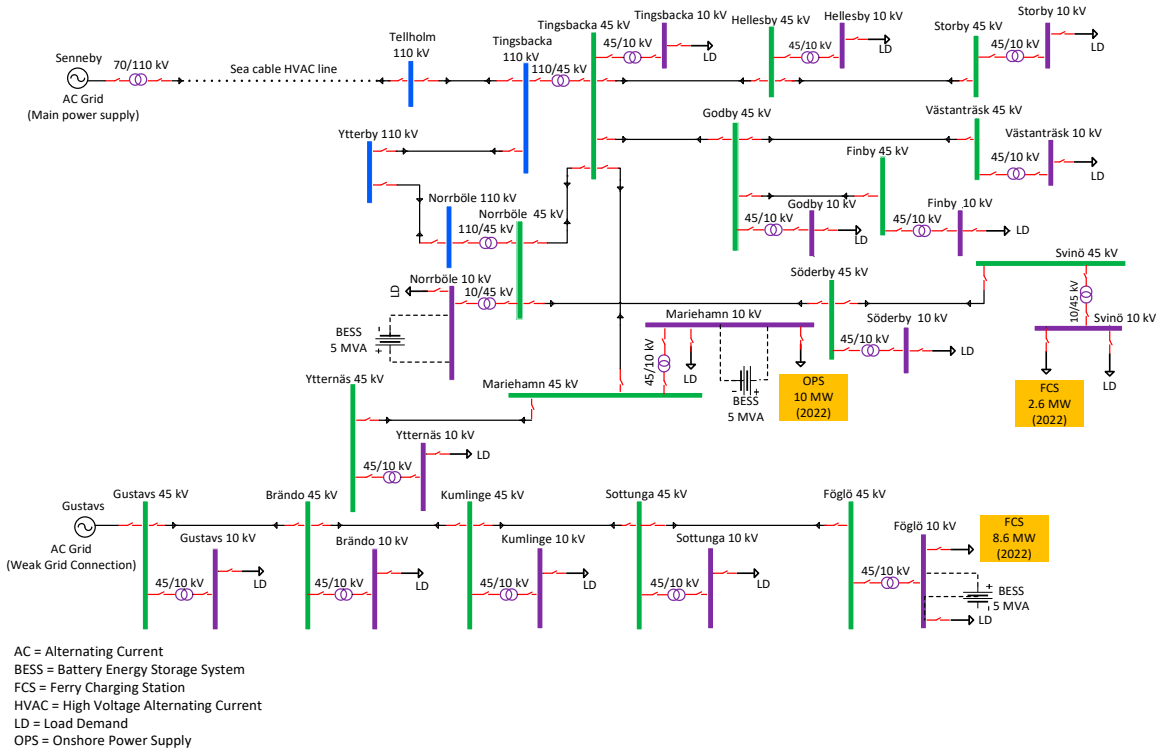


Figure 11. Radial mode operation of the Åland Islands' power system for the year 2022 with BESSs.

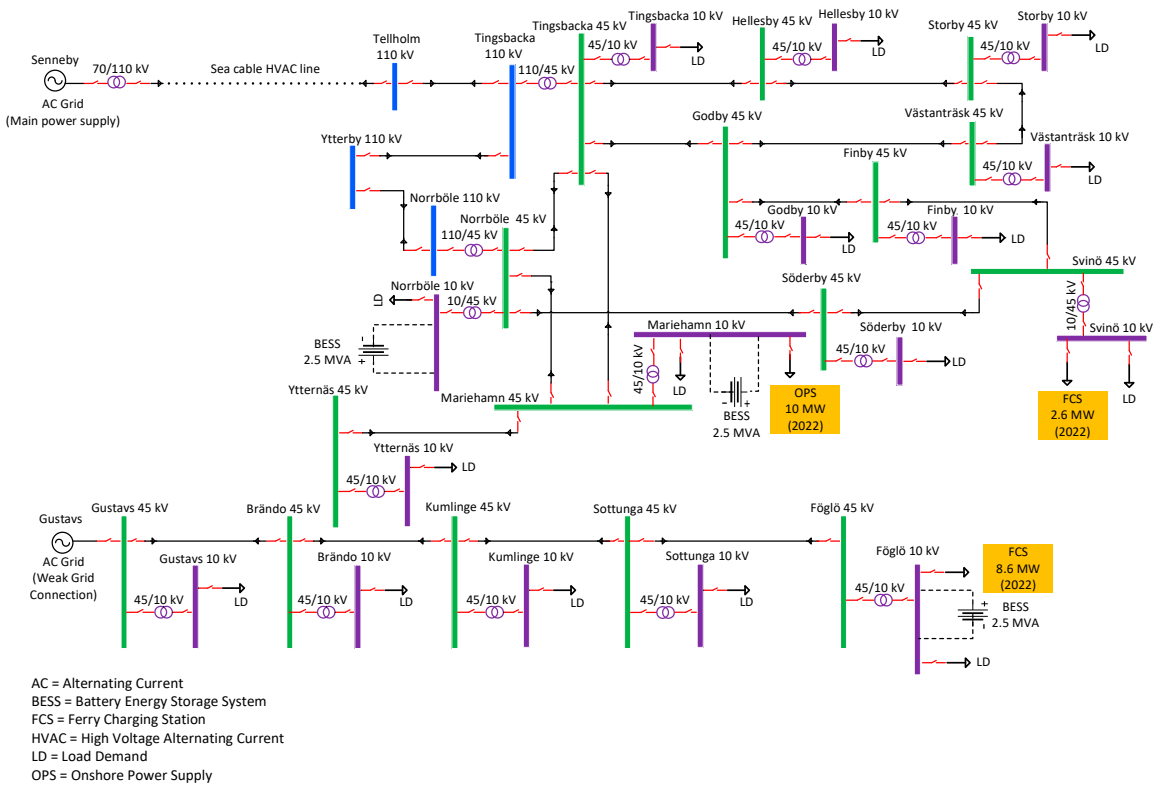


Figure 12. Meshed mode operation of the Åland Islands' power system for the year 2022 with BESSs.

Figure 14 presents the nominal current-carrying capacity of transmission lines and the operational currents of transmission lines without BESSs and with BESSs in radial and meshed network topologies. The simulation results validate that all the transmission lines are now within their nominal current-carrying capacity and none of the power transmission lines are overloaded.

3.2.3. Case 2: Year 2030 with BESSs

In the case of 2030, BESSs have also been located in two network topologies: one is the practical operating scenario—i.e., the radial network—and the other is a meshed network by considering the upper islanded network being supplied. Moreover, two islanded networks supplied from Senneby and Gustavs have also been meshed in order to reduce the size of the BESS. Figure 15 shows the radial network topology with the total predicted increase in load demand of 48.7 MW with reference to the existing load demand, and this has been distributed at Mariehamn, Svinö, Föglö, Finby, Brändo, and Kumlinge substations. In this network topology, the appropriate size and location of the BESS was determined to be as follows: 20 MVA at Mariehamn substation, 7.5 MVA at Norrböle substation, and 5 MVA at Föglö substation. Figure 16 illustrates the meshed network topology with the same increase in load demand of 48.7 MW, distributed at the above-mentioned substations. In this network topology, the suitable size and location of the BESSs was found to be 10 MVA each at Mariehamn and Norrböle substations, and 5 MVA at Föglö substation. Figure 17 shows the nominal voltage profiles of 45 kV substations and operating voltages without BESSs and with BESSs in radial and meshed network topologies. The simulation results show that the voltage profiles have somewhat improved with the integration of BESSs, and they are within the limits of ±10%. Figure 18 presents the nominal current-carrying capacity of transmission lines and the operational currents of transmission lines without BESSs and with BESSs in radial and meshed network topologies. The results verify that all the transmission lines are now within their nominal current-carrying capacity and none of the power transmission lines are overloaded.

3.3. Discussion

The findings of the present study suggest that weak electricity networks with multiple medium-size/small harbour areas require more power and energy capacity to deal with the higher power requirements of modern ships/ferries and other electrical loads at harbours. These higher power requirements of charging stations in harbours can either be accomplished by additional power supplied to harbour grids from the main grids or local power generated from renewables or BESSs. The power system in the Åland Islands has a significant potential for generating electricity locally from renewables and plans to integrate a certain amount of power from wind and photovoltaics sources in 2022 and 2030. This requires huge investments in network capacity enhancements to accommodate the additional power capacity and will cause power fluctuations due to the penetration of renewable energy resources which are intermittent in nature. Therefore, designing a relevant size and location of BESSs is necessary for such a weak network consisting of a massive amount of renewable power generation and electric ferry/ship charging stations. Short-term fluctuations are handled by the present-day Li-ion BESSs, acting as flexible energy sources, and they store energy during off-peak hours, improving the power quality and reliability of the network. This allows the shaving-off of peak loads in the network, consequently reducing voltage drops across the network, and optimising the size and infrastructure cost of passive components such as transformers, transmission lines, etc. This paper investigates the technical advantages of the proper sizing and allocation of BESSs in harbour grids for the Åland Islands' power system. However, an economic analysis of the cost savings of transformers and other equipment owing to the deferral of increasing power capacity against the net battery costs is beyond the scope of the paper.

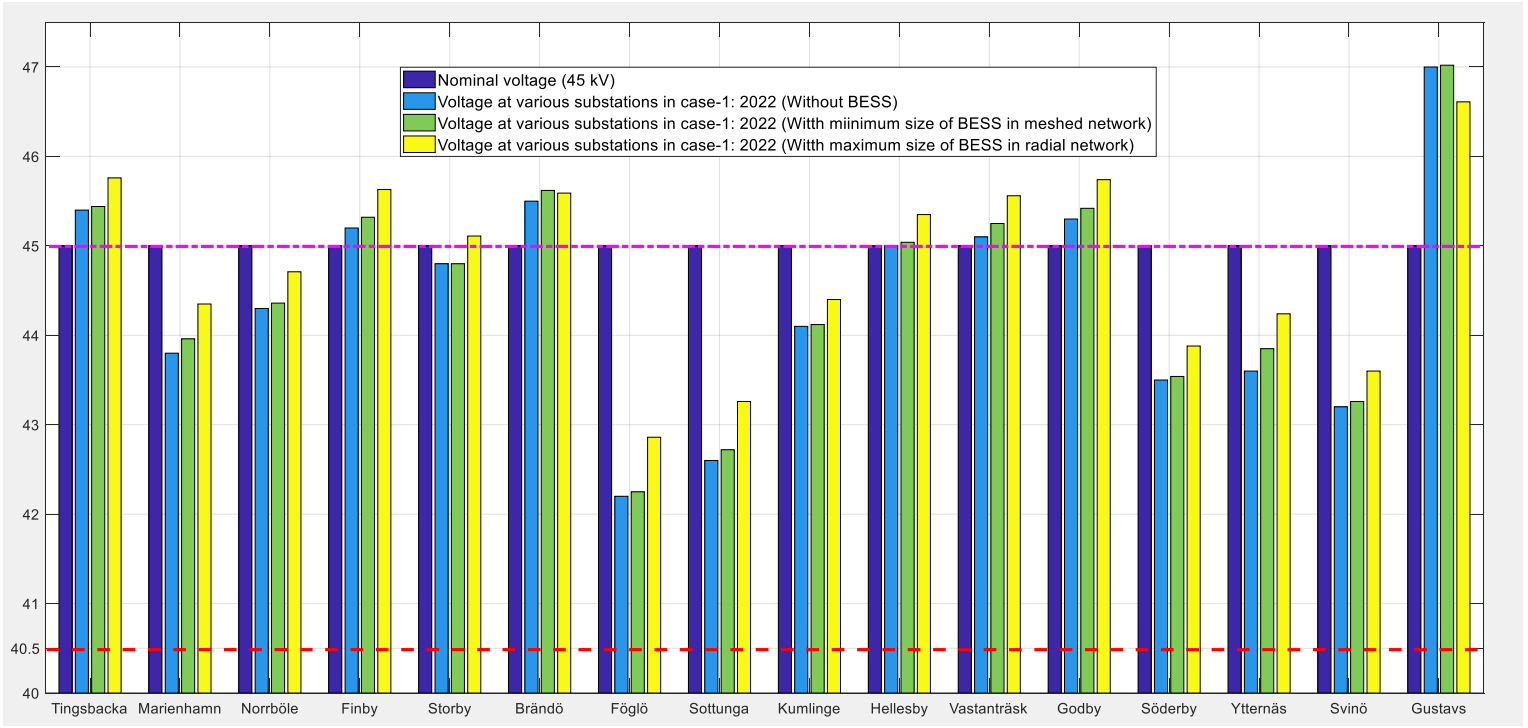


Figure 13. Nominal and operating voltages at the substations for the year 2022 with BESSs.

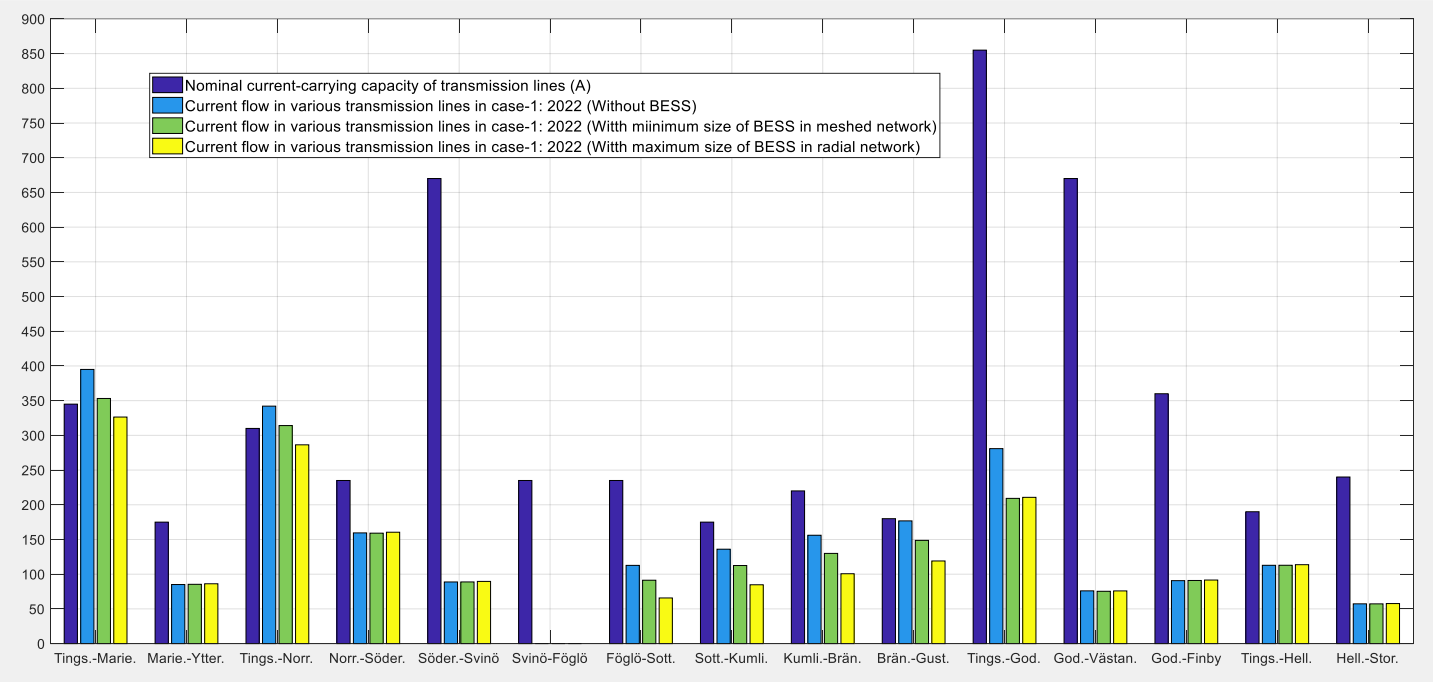


Figure 14. Nominal and actual current flows in transmission lines for the year 2022 with BESSs.

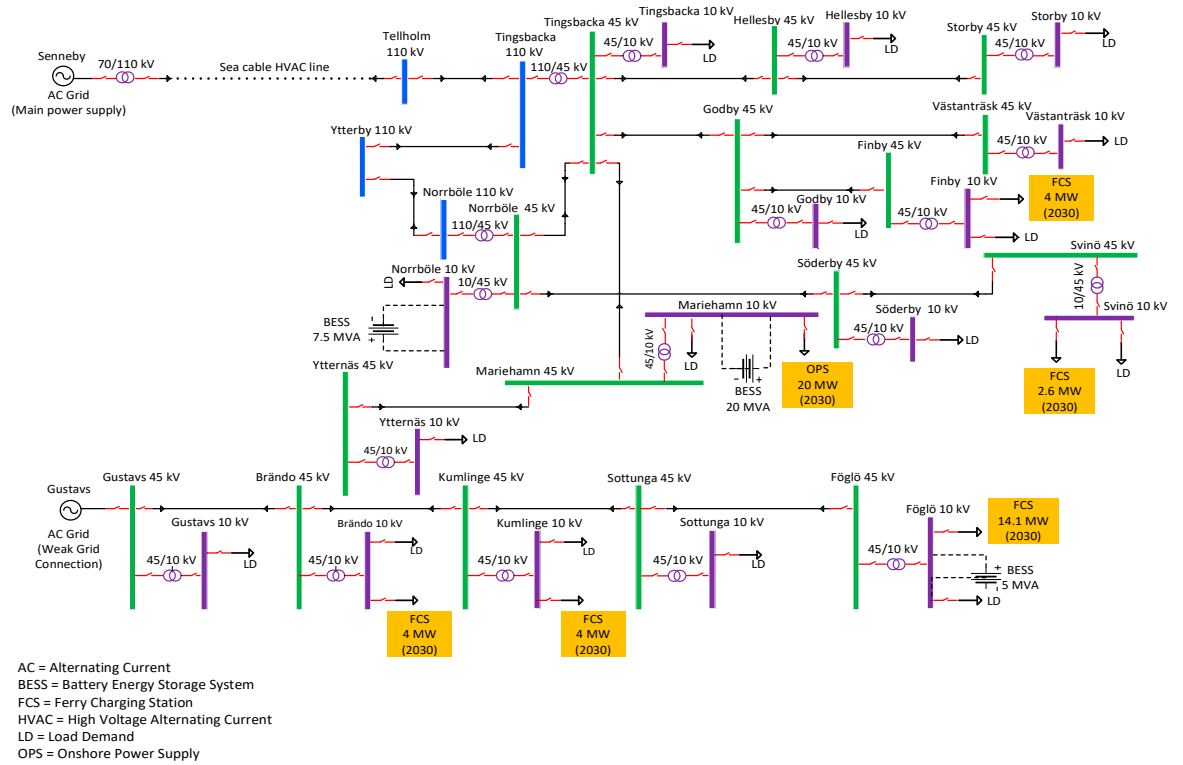


Figure 15. Radial mode operation of the electricity network in the Åland Islands for the year 2030 with BESSs.

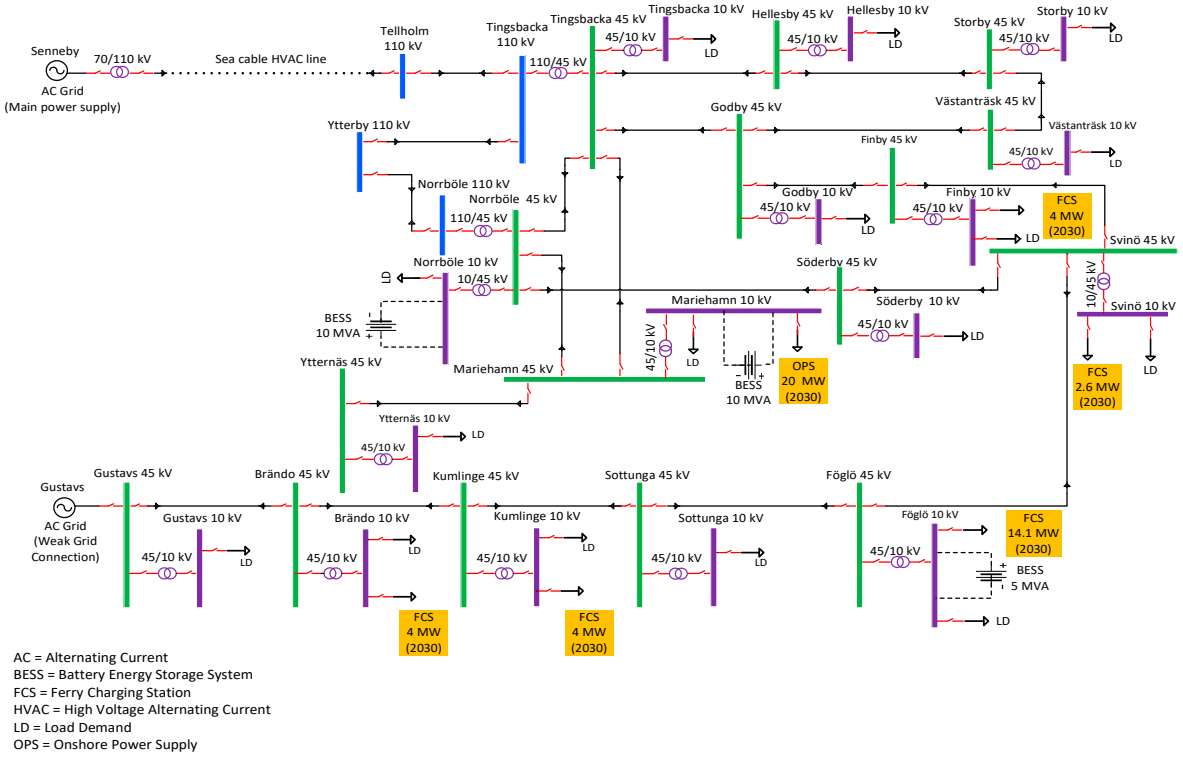


Figure 16. Meshed mode operation of the electricity network in the Åland Islands for the year 2030 with BESSs.

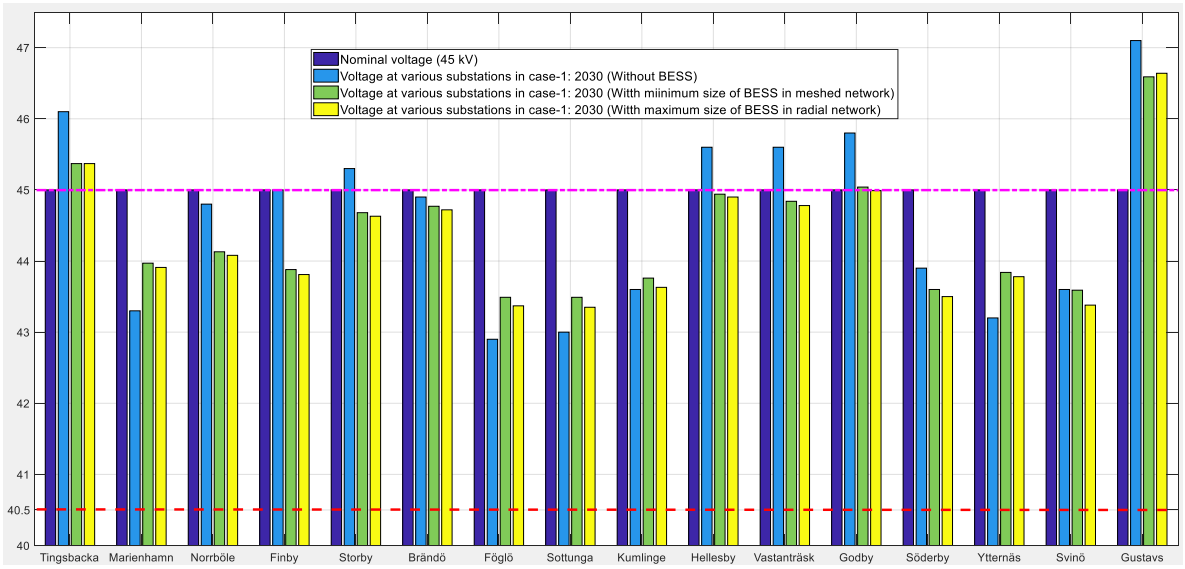


Figure 17. Nominal and operating voltages at the substations for the year 2030 with BESSs.

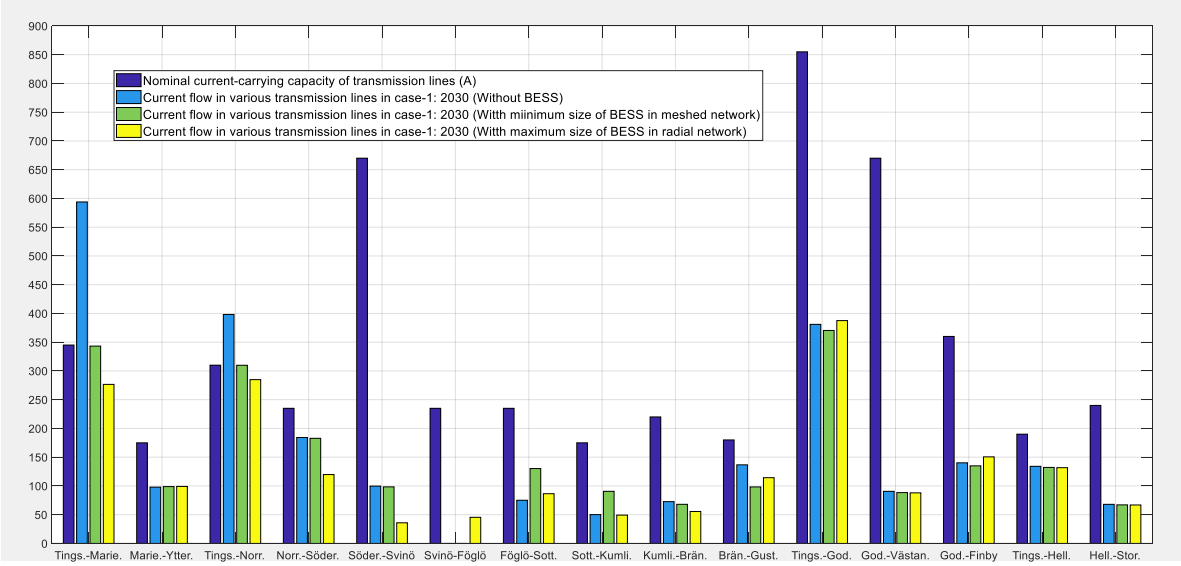


Figure 18. Nominal and actual current flows in transmission lines for the year 2030 with BESSs.

The simulation results of the power system in the Åland Islands illustrate that designing a proper size of BESSs and allocating them at appropriate substations can reduce the overcurrent flowing in certain transmission lines as well as avoid the additional cost of increasing the current-carrying capacity of transmission lines between Tingsbacka–Mariehamn and Tingsbacka–Norrböle. Besides this, Table 2 presents the transformers at various substations which need to be upgraded if BESSs are not installed for the investigated case studies of the years 2022 and 2030. In order to avoid this upgradation of transmission lines, transformers and other grid components, Table 3 summaries the required sizing and appropriate locations of batteries for future case studies of 2022 and 2030. It has been found that the meshed networks, as compared to currently operating radial network, can reduce the size and cost of the BESSs. Besides this, the meshed network can change the operational paradigm by improving the power quality and reliability of the harbour grid in the Åland Islands. However, the meshed networks bring new challenges such as an increase in the complexity of the network and operation of protection relays. The weak power system in the Åland Islands might be threaten power system transient stability issues due to the outage of one of the renewable power plants integrated at one or several locations.

Table 2. Transformer power capacity upgrades at various locations without BESSs.

Substation	Power Capacity of Transformer (MVA)		Upgrade Year
	At Present	Required in Future without BESS	
Västantrask	5	6.3	2022
Söderby	5	6.3	2022
Föglö	–	16	2030
Finby	6.3	10	2030
kumlinge	3	6.3	2030
Brändö	3	5	2030

Table 3. Sizing and Locations of BESS for 2022 and 2030.

Locations	Battery Size Required in 2022 (MVA)		Battery Size Required in 2030 (MVA)	
	Radial Topology	Meshed Topology	Radial Topology	Meshed Topology
Mariehamn	2.5	5	20	10
Nörrbole	2.5	5	7.5	10
Föglö	2.5	5	5	5

4. Conclusions

This paper has focused on the proper sizing and allocation of BESSs for harbours in weak power systems which plan to integrate RESs and electric ferry/ship charging stations into an existing electrical network. Since power from renewable energy resources is volatile, the accurate sizing and installation of the BESSs at proper locations are necessary as they can reduce the peak load demand, avoid the expansion of the existing capacities of transmission lines, and defer capital investment in other electrical equipment. The maximum current-carrying capacity, along with the operational currents in all transmission lines obtained from the simulation of the detailed PSCAD grid model, are fed to the algorithm developed in MATLAB/Simulink to obtain a proper size of BESSs at suitable locations. Moreover, the developed algorithm has been tested by taking existing original field data of the weak power system in the Åland Islands, and the results validate that the size and locations of the BESSs are accurate enough to cope with the maximum load demand considered in the case studies of 2022 and 2030 without overloading any transmission line. Congestions in the network as well as the upgrading of network components (transmission lines, transformers, and protection schemes) for the future scenarios of 2022 and 2030 could be avoided by integrating a suitable size of BESSs at certain locations. The simulation cases with a minimum sizing of batteries can reduce the peak load demand of the network, but the few line currents are near to the maximum allowed capacity limits. However, in practical operating scenarios, the maximum sizing of batteries is required, and the simulation results show that all the line currents are below the operating limits for every line.

The authors are interested in investigating other challenging tasks for future studies, such as power system protection, which is typically more challenging in meshed networks. Besides this, the power system in the Åland Islands might be at risk of transient stability issues due to the variable nature of the new low-inertia renewable power plants integrated at one or several locations. Therefore, in future, the power system stability and the role of BESSs in mitigating issues should be carefully studied. In future studies, the effect of battery sizing and location, while considering accurate profiles of power production from renewable energy sources, will be evaluated. Studies related to batteries at different stages to evaluate the role of battery aging in designing control strategies of BESSs in harbour area smart grids will also be considered for future research.

Author Contributions: Conceptualization, J.K. and C.P.; Methodology, C.P. and J.K.; Software, J.K., C.P., and M.V.; Validation, J.K., C.P. and M.V.; Formal analysis, H.L., M.S.-K. and K.K.; Funding acquisition, H.L. Investigation, H.L., M.S.-K.; Writing—original draft preparation, J.K. and C.P.; Writing—review and editing, H.L., M.S.-K. and K.K.; Visualization, J.K., C.P. and H.L.; Supervision, H.L. and K.K.; Project administration, H.L. All authors have read and agreed to the published version of the manuscript.

Funding: This work was supported by the FLEXe-demo project funded by CLIC Innovation Oy. The corresponding author is also thankful to the University of Vaasa for a grant of a doctoral position to carry out this research.

Conflicts of Interest: The authors declare no conflict of interest.

Abbreviations

AC	Alternating current
BESS	Battery energy storage system
DC	Direct current
DG	Distributed generation
ECM	Equivalent circuit model
KBM	Kinetic battery model
Li-ion	Lithium-ion
NMC	Nickel–cobalt–manganese-oxide
PSCAD	Power Systems Computer-Aided Design
PV	Photovoltaic
RC	Resistive–capacitive
RES	Renewable energy source
SoC	State of Charge
SOEC	Second-order equivalent circuit
VSC	Voltage source converter

References

1. International Maritime Organization. *Third IMO GHG Study 2014 Executive Summary and Final Report*; International Maritime Organization: London, UK, 2015.
2. Kumar, J.; Kumpulainen, L.; Kauhaniemi, K. Technical design aspects of harbour area grid for shore to ship power: State of the art and future solutions. *Int. J. Electr. Power Energy Syst.* **2019**, *104*, 840–852. [CrossRef]
3. Peralta, P.C.; Vieira, G.; Meunier, S.; Vale, R.; Salles, M.; Carmo, B. Evaluation of the CO2 Emissions Reduction Potential of Li-ion Batteries in Ship Power Systems. *Energies* **2019**, *12*, 375. [CrossRef]
4. Kumar, J.; Palizban, O.; Kauhaniemi, K. Designing and analysis of innovative solutions for harbour area smart grid. In Proceedings of the 2017 IEEE Manchester PowerTech, Manchester, UK, 18–22 June 2017; IEEE: Piscataway, NJ, USA, 2017; pp. 1–6.
5. Official Journal of the European Union. *Directive 2005/33/EC Of the European Parliament and of the Council*; Official Journal of the European Union: Brussels, Belgum, 2005.
6. Fang, S.; Wang, Y.; Gou, B.; Xu, Y. Towards Future Green Maritime Transportation: An Overview of Seaport Microgrids and All-electric Ships. *IEEE Trans. Veh. Technol.* **2019**, 1. [CrossRef]
7. Lee, K.-J.; Shin, D.; Yoo, D.-W.; Choi, H.-K.; Kim, H.-J. Hybrid photovoltaic/diesel green ship operating in standalone and grid-connected mode—Experimental investigation. *Energy* **2013**, *49*, 475–483. [CrossRef]
8. Kumar, J.; Devi, J.; Mustafa, G.; Parveen, S.; Shafiq, M. Analysis of Spatially Modelled High Temperature Polymer Electrolyte Membrane Fuel Cell under Dynamic Load Conditions. *Int. J. Adv. Comput. Sci. Appl.* **2019**, *10*. [CrossRef]
9. Hansen, J.F.; Wendt, F. History and State of the Art in Commercial Electric Ship Propulsion, Integrated Power Systems, and Future Trends. *Proc. IEEE* **2015**, *103*, 2229–2242. [CrossRef]
10. Mutarraf, M.U.; Terriche, Y.; Niazi, K.A.K.; Vasquez, J.C.; Guerrero, J.M. *Energy Storage Systems for Shipboard Microgrids—A Review*; MDPI: Basel, Switzerland, 2018; Volume 11, ISBN 4591778118.
11. Al-Falahi, M.; Tarasiuk, T.; Jayasinghe, S.; Jin, Z.; Enshaei, H.; Guerrero, J. AC Ship Microgrids: Control and Power Management Optimization. *Energies* **2018**, *11*, 1458. [CrossRef]

12. Babaei, M.; Shi, J.; Abdelwahed, S. A Survey on Fault Detection, Isolation, and Reconfiguration Methods in Electric Ship Power Systems. *IEEE Access* **2018**, *6*, 9430–9441. [CrossRef]
13. Kumar, J.; Memon, A.A.; Kumpulainen, L.; Kauhaniemi, K.; Palizban, O. Design and Analysis of New Harbour Grid Models to Facilitate Multiple Scenarios of Battery Charging and Onshore Supply for Modern Vessels. *Energies* **2019**, *12*, 2354. [CrossRef]
14. Gennitsaris, S.; Kanellos, F.D. Emissions-Aware and Cost-Effective Distributed Demand Response System for Extensively Electrified Large Ports. *IEEE Trans. Power Syst.* **2019**, *34*, 4341–4351. [CrossRef]
15. Kanellos, F.D.; Volanis, E.S.M.; Hatziargyriou, N.D. Power management method for large ports with multi-agent systems. *IEEE Trans. Smart Grid* **2019**, *10*, 1259–1268. [CrossRef]
16. Kim, Y.; Song, Y.; Lim, S.H. Hierarchical Maritime Radio Networks for Internet of Maritime Things. *IEEE Access* **2019**, *7*, 54218–54227. [CrossRef]
17. Lamberti, T.; Sorce, A.; Di Fresco, L.; Barberis, S. Smart port: Exploiting renewable energy and storage potential of moored boats. In Proceedings of the OCEANS 2015—Genova, Genoa, Italy, 18–21 May 2015; IEEE: Piscataway, NJ, USA, 2015; pp. 1–3.
18. Parise, G.; Parise, L.; Martirano, L.; Ben Chavdarian, P.; Chun-Lien, S.; Ferrante, A. Wise Port and Business Energy Management: Port Facilities, Electrical Power Distribution. *IEEE Trans. Ind. Appl.* **2016**, *52*, 18–24. [CrossRef]
19. Pavlic, B.; Cepak, F.; Sucic, B.; Peckaj, M.; Kandus, B. Sustainable port infrastructure, practical implementation of the green port concept. *Therm. Sci.* **2014**, *18*, 935–948. [CrossRef]
20. Nikitakos, N. Green logistics—The concept of zero emissions port. *FME Trans.* **2012**, *40*, 201–206.
21. Kanellos, F.D. Real-Time Control Based on Multi-Agent Systems for the Operation of Large Ports as Prosumer Microgrids. *IEEE Access* **2017**, *5*, 9439–9452. [CrossRef]
22. Parthasarathy, C.; Hafezi, H.; Laaksonen, H.; Kauhaniemi, K. Modelling and Simulation of Hybrid PV & BES Systems as Flexible Resources in Smartgrids–Sundom Smart Grid Case. In Proceedings of the IEEE PES PowerTech Conferences, Milan, Italy, 23–27 June 2019; IEEE: Piscataway, NJ, USA, 2019; pp. 1–6.
23. Wong, L.A.; Ramachandaramurthy, V.K.; Taylor, P.; Ekanayake, J.B.; Walker, S.L.; Padmanaban, S. Review on the optimal placement, sizing and control of an energy storage system in the distribution network. *J. Energy Storage* **2019**, *21*, 489–504. [CrossRef]
24. Yang, Y.; Bremner, S.; Menictas, C.; Kay, M. Battery energy storage system size determination in renewable energy systems: A review. *Renew. Sustain. Energy Rev.* **2018**, *91*, 109–125. [CrossRef]
25. Chauhan, P.J.; Reddy, B.D.; Bhandari, S.; Panda, S.K. Battery energy storage for seamless transitions of wind generator in standalone microgrid. *IEEE Trans. Ind. Appl.* **2019**, *55*, 69–77. [CrossRef]
26. Tariq, M.; Maswood, A.I.; Gajanayake, C.J.; Gupta, A.K. Modeling and Integration of a Lithium-Ion Battery Energy Storage System With the More Electric Aircraft 270 V DC Power Distribution Architecture. *IEEE Access* **2018**, *6*, 41785–41802. [CrossRef]
27. Bako, Z.N.; Tankari, M.A.; Lefebvre, G.; Maiga, A.S. Experiment-based methodology of kinetic battery modeling for energy storage. *IEEE Trans. Ind. Appl.* **2019**, *55*, 593–599. [CrossRef]
28. El Sayed, M.; Ahmed, R.; Habibi, S.; Jimi, T.; Arasaratnam, I. Reduced-Order Electrochemical Model Parameters Identification and SOC Estimation for Healthy and Aged Li-Ion Batteries Part I: Parameterization Model Development for Healthy Batteries. *IEEE J. Emerg. Sel. Top. Power Electron.* **2014**, *2*, 659–677.
29. Min Chen, G.A.R. An Accurate Electrical Battery Model Capable of Predicting Lifetime and I–V Performance Motivation. *IEEE Trans. Energy Convers.* **2006**, *21*, 1–8.
30. Nadeau, J.; Dubois, M.R.; Desrochers, A.; Denis, N. Ageing estimation of lithium-ion batteries applied to a three-wheel PHEV roadster. In Proceedings of the 2013 9th IEEE Vehicle Power and Propulsion Conference (VPPC), Beijing, China, 15–18 October 2013; IEEE: Piscataway, NJ, USA; pp. 49–54.
31. Deng, Z.; Deng, H.; Yang, L.; Cai, Y.; Zhao, X. Implementation of reduced-order physics-based model and multi-parameters identification strategy for lithium-ion battery. *Energy* **2017**, *138*, 509–519. [CrossRef]
32. Lawder, M.T.; Suthar, B.; Northrop, P.W.C.; De, S.; Hoff, C.M.; Leitermann, O.; Crow, M.L.; Santhanagopalan, S.; Subramanian, V.R. Battery energy storage system (BESS) and battery management system (BMS) for grid-scale applications. *Proc. IEEE* **2014**, *102*, 1014–1030. [CrossRef]
33. Arunachala, R.; Parthasarathy, C.; Jossen, A.; Garche, J. Inhomogeneities in large format lithium ion cells: A study by battery modelling approach. *ECS Trans.* **2016**, *73*, 201–212. [CrossRef]

34. Meng, J.; Luo, G.; Ricco, M.; Swierczynski, M.; Stroe, D.-I.; Teodorescu, R. Overview of Lithium-Ion Battery Modeling Methods for State-of-Charge Estimation in Electrical Vehicles. *Appl. Sci.* **2018**, *8*, 659. [CrossRef]
35. Geogrhical Location and Electrical Network of Åland Islands. Available online: http://www.kraftnat.ax/text2.con?iPage=28&iLan=1 (accessed on 18 October 2019).



© 2020 by the authors. Licensee MDPI, Basel, Switzerland. This article is an open access article distributed under the terms and conditions of the Creative Commons Attribution (CC BY) license (http://creativecommons.org/licenses/by/4.0/).